Available online at www.sciencedirect.com
SCIENCE DIRECT®

Journal of the European Ceramic Society 23 (2003) 2177–2181
www.elsevier.com/locate/jeurceramsoc

Modeling and analysis of the electrical properties of PZT through neural networks

Dong Guo[a,*], Longtu Li[a], Cewen Nan[a], Juntao Xia[b], Zhilun Gui[a]

[a]*Department of Materials Science & Engineering, Tsinghua University, 100084 Beijing, PR China*
[b]*School of Chemical Engineering and Materials, Beijing Institute of Technology, 100081 Beijing, PR China*

Received 20 September 2002; accepted 3 December 2002

Abstract

Application of ANN (Artificial neural network) to the electrical properties analysis of PZT is discussed in this paper. The same set of results of PZT samples were analyzed by a back-propagation (BP) network in comparison with a multiple nonlinear regression analysis (MNLR) model. The results revealed that the ANN model is much more accurate than MNLR model. The ANN approach also gave quite encouraging predictions for formulations not included in the train set samples, indicating that the BP network is a very useful and accurate tool for the properties analysis and prediction of multi-component solid solution piezoelectric ceramics.
© 2003 Elsevier Science Ltd. All rights reserved.

Keywords: Neural networks; BP algorithm; Piezoelectric properties; PZT; Modeling

1. Introduction

Piezoelectric materials find increasing demand in a wide field of applications such as actuators and transducers etc. within the last several decades. In order to satisfy different requirements and to enhance the performance of this kind of materials, addition of different dopants is an intensively used modification approach. The ever-increasing need of materials with all-around excellent performance often makes it necessary to use multi-component solid solution system. Although the effects of a variety of doping elements on the electrical properties of piezoelectric material have been investigated, it is usually difficult to discover ceramic formulation that can satisfy all the serious requirements and sometimes it is difficult to explain the action of a new additive, especially in the complicated solid solution system. For this purpose, developing a reliable modeling for the ceramic compounding seems to be very helpful.

Due to its remarkable information processing characteristics such as non-linearity, high parallelism, robustness, fault and failure tolerance, learning, ability to handle imprecise and fuzzy information, and the capability to generalize, ANN has been extensively utilized in solving a diverse areas of science and engineering problems.[1] However, very few is known of the application of this technique to the investigation of complicated ceramic materials. In our previous paper, the correlation between some electrical parameters and components for $BaTiO_3$ based dielectric materials has been delineated based on ANN method.[2] PZT is one of the most widely investigated piezoelectric systems. The goal of this paper concerns with the properties analysis and prediction of PZT type ceramics. The same set of experiment data were also used to develop a MNLR model in order to compare the accuracy of ANN with the conventional method. Most importantly, several formulations not included in the train set were also tested and quite encouraging predictions were obtained.

2. Experimental procedure

2.1. Materials preparation and measurement

There are mainly two types of dopants for PZT, i.e., the donor type (soft type) and the acceptor type (hard

* Corresponding author. Fax: +86-10-6277-1160.
E-mail address: guodong99@mails.tsinghua.edu.cn (D. Guo).

0955-2219/03/$ - see front matter © 2003 Elsevier Science Ltd. All rights reserved.
doi:10.1016/S0955-2219(03)00020-7

type). Donor doping can provide a higher electromechanical coupling coefficient and piezoelectric coefficient and a lower mechanical quality factor and electrical quality factor etc. While the role of the acceptor doping is just on the contrary. Thereby in order to increase the piezoelectric coefficient of PZT two donor type dopants, Nb_2O_5 and La_2O_3, were selected. Another seldom investigated B site (Zr, Ti) isovalent dopant CeO_2 that can't belong to both doping types was also selected. At near the morphotropic phase boundary (MPB) composition (Zr/Ti≈52/48) a series of properties of PZT can be substantially affected by the Zr/Ti ratio, thus ZrO_2 and TiO_2 were also set as variables and the contents of the two components were set near the MPB boundary. To maintain a stoichiometrically total amount of $PbZrO_3$ and $PbTiO_3$, the upper limit and lower limit of ZrO_2 and TiO_2 were set contrarily. Besides, firing temperature was also considered as a variable of the formulation. The addition levels of each additives and the temperature range are listed in Table 1, where the maximum content of La_2O_3, Nb_2O_5 and CeO_2 are about 3 mol%, 2 mol% and 2.5 mol% respectively.

21 formulations derived from homogenous experimental design tables were used as the training data set for knowledge acquisition.[3] In each formulation 1.5% excess Pb_3O_4 was used in case of the Pb loss during firing of the powders, and the Pb_3O_4 content was fixed as 20.3 g. Pb_3O_4, ZrO_2, TiO_2, Nb_2O_5, La_2O_3 and CeO_2 were weighed, mixed in ethanol and thoroughly ball-milled for 24 h. After drying the mixture was fired, then the synthesized powder was pressed into disks with a diameter of about 15 mm and a thickness of about 1 mm. After being sintered at 1260 °C for 3 h the ceramic disks were paved with Ag-electrode and polarized in a silicon oil bath by applying an electric field of 3 kV/mm at 120 °C for 30 min. Piezoelectric coefficient d_{33} of the samples were determined by using a ZJ-3A piezometer. Electromechanical coupling coefficient K_p and dielectric loss tangent tgδ were measured by a HP4194A impedance analyzer. Remnant polarization P_r of the samples were measured by using a RT6000HVS ferroelectric test system (Radiant Technology Incorporation, USA). The ultimate results are listed in Table 2.

2.2. ANN modeling of the PZT system

The ANN employed here is a BP network consisting of three layers. The first layer is the input layer with nodes representing input variables to the problem (e.g. dopant content or temperature). The last layer is the output layer with nodes representing the dependent variables (e.g. d_{33} calculated). Between them is a hidden layer containing nodes to help capture the non-linearity of the data. Both input and hidden layers have an additional bias neuron. Different layers are connected by weights. Because Pb_3O_4 content is fixed, the ANN model is composed of six neurons in the input layer and four neurons in the output layer. After several trials of different numbers of hidden neurons, eight neurons were selected in the hidden layer. Therefore the structure of the ANN model for the PZT formulation can be shown as Fig. 1. The results shown in Table 2 were used as the training data set for the ANN model. Because a value near 0 or 1 will lead to the "inaction" of the network, the input data (all in g) and the output data in Table 2 were normalized to give values between around 0.05 and 0.95 prior to training.[2] The ANN is built by repeatedly adjusting weights until the overall error between calculated and target outputs is approaching to the preset error criteria. The detailed steps of the BP algorithm performed in the network was reported elsewhere.[2] Some parameters of the ANN model are listed in Table 3. Within the neural network the learning rate η, the momentum μ and the convergence error are all empirical values. A high η will accelerate training by changing the weight significantly from one cycle to another. However, this may cause the search to oscillate on the error surface and never converge, thus increasing the risk of overshooting a near-optimal weight. Whereas a small η drives the search steadily, though slowly. A high μ will reduce the risk of the network being stuck in local minima, but it increases the risk of overshooting the solution as does a high η. Too small a convergence error will result in overfitting of the model.

3. Results and discussion

3.1. Prediction capability of the ANN model

The finished ANN model is delineated by the connection weights between the input and hidden layers and the connection weights between the hidden and output layers, which are listed in Tables 4 and 5 respectively. In order to compare the accuracy between ANN method and MNLR method, the same data in Table 2 were also used to develop MNLR model for correlations between the properties and the formulations. As an example, the model of d_{33} can be expressed in Eq. (1).

Table 1
Dopants addition levels and firing temperature range (Pb_3O_4 is a constant of 20.3 g)

Dopant	ZrO_2 (g)	TiO_2 (g)	Nb_2O_5 (g)	La_2O_3 (g)	CeO_2 (g)	Temp. (°C)
Lower limit	5.36	3.52	0	0	0	800
Upper limit	5.84	3.2	0.36	0.32	0.2	1000

Table 2
Experimental results of 21 PZT samples

Sample							
	PZT-1	PZT-2	PZT-3	PZT-4	PZT-5	PZT-6	PZT-6
d_{33} (pC/N)	342	302	297	270	182	339	399
tgδ	0.0169	0.0189	0.02	0.0169	0.0349	0.0167	0.0202
K_p	0.573	0.541	0.516	0.346	0.330	0.587	0.626
P_r (μC/cm^2)	18.8	14.1	6.3	22.2	32.7	33.2	24.6
	PZT-8	PZT-9	PZT-10	PZT-11	PZT-12	PZT-13	PZT-14
d_{33} (pC/N)	298	296	284	372	398	345	363
tgδ	0.0192	0.0182	0.0217	0.0468	0.0194	0.0255	0.0208
K_p	0.542	0.496	0.493	0.544	0.643	0.540	0.601
P_r (μC/cm^2)	22.9	21.7	15.1	14.7	39.1	23	41.9
	PZT-15	PZT-16	PZT-17	PZT-18	PZT-19	PZT-20	PZT-21
d_{33} (pC/N)	315	389	358	401	352	329	286
tgδ	0.0258	0.0271	0.0253	0.0217	0.0455	0.0187	0.0292
K_p	0.494	0.644	0.587	0.641	0.578	0.563	0.481
P_r (μC/cm^2)	21	38.3	26.8	30	28.9	30.6	20.8

Table 3
Critical parameters of the PZT BP network

Neuron function	Learning rate η	Momentum factor μ	Range of initial weights	Maximum iterations	Convergence error
Sigmoid function	0.15	0.95	−0.3∼0.3	5000	0.01

$$\begin{aligned} d_{33} = {} & 16996.20 + 200.95 \times ZrO_2 - 6803.79 \times TiO_2 \\ & + 40224.69 \times Nb_2O_5 + 3935.94 \times La_2O_3 \\ & + 76125.29 \times CeO_2 + 0.90 \times Temp - 11007.65 \\ & \times Nb_2O_5 \times La_2O_3 + 1486.82 \times Nb_2O_5 \times CeO_2 \\ & - 20292.84 \times La_2O_3 \times CeO_2 - 31.17 \times Nb_2O_5 \\ & \times Temp - 0.20 \times La_2O_3 \times Temp - 60.26 \\ & \times CeO_2 \times Temp \end{aligned}$$

where the additives are all expressed in g and three reciprocal effects of the three dopants, i.e. $Nb_2O_5 \times La_2O_3$, $Nb_2O_5 \times CeO_2$ and $La_2O_3 \times CeO_2$, and three reciprocal effects between each dopant and temperature were considered.

Table 4
Connection weights between the input and hidden layers

	ZrO_2	TiO_2	Nb_2O_5	La_2O_3	CeO_2	Temp.	Input bias
h_1	−3.693	−2.236	3.890	1.511	−2.704	3.140	−2.237
h_2	−4.492	2.544	−1.066	−1.502	2.698	−0.776	−5.011
h_3	−1.442	−4.398	−1.582	0.566	0.357	3.687	3.637
h_4	4.202	−4.332	2.001	−0.191	−3.640	4.096	−0.845
h_5	1.259	0.540	−0.368	−1.342	0.481	0.544	−2.867
h_6	6.233	1.385	−0.606	−3.784	−0.298	−2.031	−1.570
h_7	5.619	−0.040	−0.703	−4.099	0.018	−1.066	2.642
h_8	0.489	2.226	1.942	−1.141	−0.047	−0.459	−2.060
h_9	2.923	−0.221	−5.009	1.095	5.174	0.131	−7.168

The prediction abilities of d_{33} values of 21 samples of both models are intuitively illustrated in Fig. 2, where the two coordinates of a point represent observed and calculated d_{33} values of a sample respectively. We can see that ANN model gives much better predictions than MNLR model. Because the accuracy of the ANN model can be increased by decreasing the convergence error, ANN model can be built more accurate than MNLR

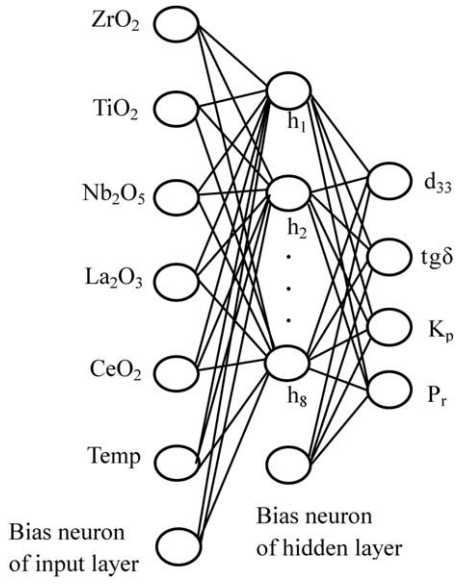

Fig. 1. Schematic view of the BP network for PZT formulation model.

Table 5
Connection weights between the hidden and output layers

	h_1	h_2	h_3	h_4	h_5	h_6	h_7	h_8	h_9	Hidden bias
d_{33}	−0.724	1.342	−1.463	3.704	−2.269	4.478	−2.019	−3.883	−1.166	1.311
tgδ	2.778	−1.412	−4.657	1.063	−7.403	−0.260	1.368	−1.224	6.146	−0.741
K_p	−2.585	−1.447	4.662	0.613	2.866	2.977	−2.030	−0.441	−2.979	−0.415
P_r	5.409	0.332	−9.075	1.283	5.513	0.620	2.258	−6.942	1.714	2.535

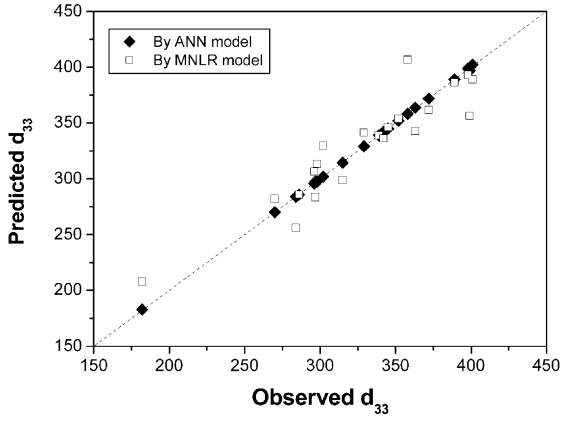

Fig. 2. Correlations between calculated and observed d_{33} of 21 samples by both ANN and MNLR model.

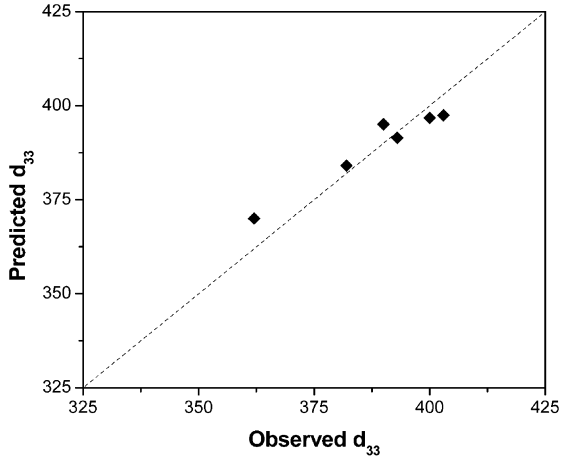

Fig. 3. Correlations between calculated and observed d_{33} for six formulations not included in the training data set.

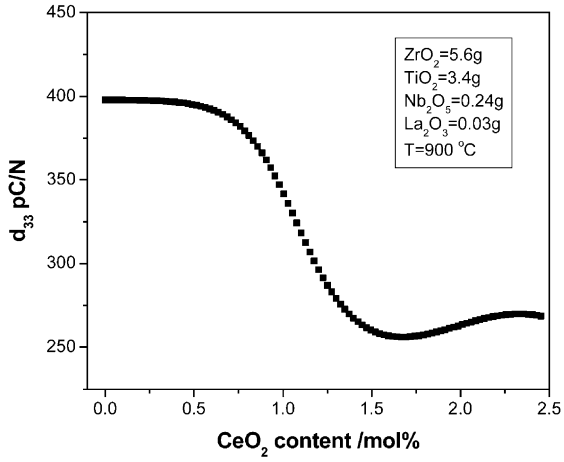

Fig. 4. Graphical analysis of the correlation between d_{33} and CeO_2.

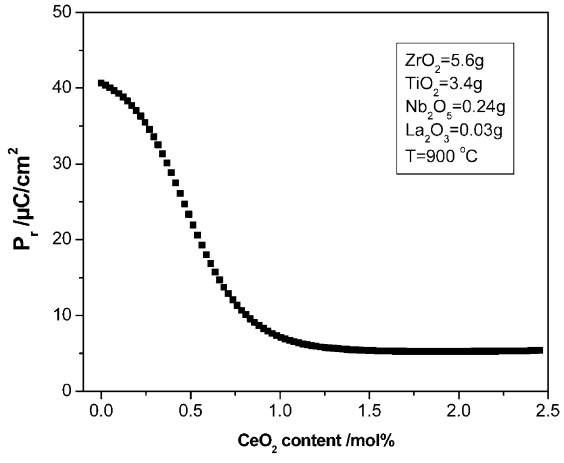

Fig. 5. Graphical analysis of the correlation between P_r and CeO_2.

model in predicting the original training formulations. However, too small a convergence error will result in overfitting of the model.[4] As a result, prediction errors for formulations not included in the training set might increase drastically. Therefore for a more convincingly inspection of the accuracy of the ANN model, six new formulations with all ingredients within the original addition levels were but different from the training samples also tested. Fig. 3 indicates that the predicted values are in good accordance with observed values for d_{33}. Prediction capability of ANN for four parameters of the new set of samples characterized through the root mean-square (RMS) error and the correlation coefficient are also listed in Table 6. Predictions of K_p and P_r are less accurate than d_{33} and tgδ, which may be ascribed to the bigger measurement errors of K_p and P_r. K_p is calculated via the resonant and anti-resonant frequencies method while P_r can be influenced by defects in the sample or on the electrode. These are further evidences for the validity of the ANN model.

Table 6
Predictive results for the new set of samples by the initially established ANN model

	d_{33}	tgδ	K_p	P_r
Correlation coefficient (R)	0.9354	0.8459	0.7145	0.7762
Root mean-square (RMS)	4.8 (pC/N)	0.0009	0.0176	4.20 (μC/cm^2)

3.2. Correlation analysis between performance and CeO_2

By using the registered ANN model, the correlation between the properties and the input variables can be conveniently derived. Influence of CeO_2 content on the d_{33} values of the PZT samples calculated by the ANN model is shown in Fig. 4. We can see that with the increase of CeO_2 d_{33} keeps almost constant initially, then it exhibits a sharp decrease. Variation of remnant polarization P_r with CeO_2 content shown in Fig. 5 exhibits similar shape. Similar phenomenon has been reported by Garg that d_{33} decrease with CeO_2 when CeO_2 exceeds 0.1 mol% in the material.[5] They ascribed this to the substitution of reduced Ce^{3+} for the B sites or immigration of Ce to the grain boundary, and the variation of the MPB boundary when the amount of CeO_2 increases. Based on our results, the sharp decrease of d_{33} and P_r might be mainly due to the variation of the MPB boundary, because near this boundary the properties of PZT can be substantially affected.

4. Conclusion

The results indicate that ANN modeling can provide highly accurate correlation with reasonable good prediction power. In combination with our previous results of applying ANN to the analysis of $BaTiO_3$ ceramics, it may be concluded that the highly non-linearity characteristic and the capability to generalize of ANN make it a very suitable tool for modeling and analysis of complex ceramic solid solution materials. The results also suggest that excess amount of CeO_2 may cause the deterioration of the piezoelectricity of the PZT.

Acknowledgements

The authors would like to thank the National Natural Science Foundation of P.R. China (Grant No. 59995523) for its financial supports.

References

1. Basheer, I. A. and Hajmeer, M., Artificial neural networks: fundamentals, computing, design, and application. *J. Micro. Meth.*, 2000, **43**, 3–31.
2. Guo, D., Wang, Y. L. and Xia, J. T. et al., Investigation of $BaTiO_3$ formulation: an artificial neural network method. *J. Eur. Ceram. Soc.*, 2002, **22**, 1867–1872.
3. Fang, K. T., *Homogeneous Design and Homogeneous Design Tables*. Science Press, Beijing, 1994.
4. Navak, B., Superfast autoconfiguring artificial neural networks and their application to power systems. *Electr. Pow. Syst. Res.*, 1995, **35**, 11–16.
5. Garg, A. and Agrawal, D. C., Structural and electrical studies of CeO_2 modified lead zirconate titanate ceramics. *J. Mater. Sci. Mater. El.*, 1999, **10**, 649–652.